chemistry

MDPI

Article

Conformational Preference of Flavonols and Its Effect on the Chemical Properties Involved in Radical Scavenging Activity

Hiroko X. Kondo [1,2,3,*] and Yu Takano [2,*]

[1] School of Regional Innovation and Social Design Engineering, Faculty of Engineering, Kitami Institute of Technology, Kitami 090-8507, Japan
[2] Department of Biomedical Information Sciences, Graduate School of Information Sciences, Hiroshima City University, Hiroshima 731-3194, Japan
[3] Laboratory for Computational Molecular Design, RIKEN Center for Biosystems Dynamics Research, Suita 565-0874, Japan
* Correspondence: h_kondo@mail.kitami-it.ac.jp (H.X.K.); ytakano@hiroshima-cu.ac.jp (Y.T.); Tel.: +81-157-26-9401 (H.X.K.); +81-082-830-1825 (Y.T.)

Abstract: Flavonols are compounds with radical-scavenging activities that can prevent the harmful effects of free radicals. Their radical-scavenging activity has attracted significant attention. Recently, quantum chemistry-based methodologies have significantly improved the understanding of the activity due to dramatic increases in computational power and software improvements. A standardized analysis method for estimating radical scavenging activity, the quantum mechanics-based test for overall free radical scavenging activity (QM-ORSA), has been proposed. An obstacle in applying the QM-ORSA protocol to flavonols is the large number of conformers and hydroxy groups for analysis. In this study, we focused on it and analyzed the conformational dependences of three flavonols (myricetin, quercetin, and kaempferol) on their chemical properties: bond dissociation energy, pK_a, and ionization energy. As a result, all chemical properties were insensitive to conformational differences. The conformational search should be performed separately for each in the gas phase and in aqueous solution because of the differences in the major conformer (relative population of each conformer). These results suggest that it is important to perform the conformational search separately in water and in the gas phase and to determine one representative structure for analyzing radical scavenging activity.

Keywords: flavonol; conformational search; bond dissociation energy; pK_a

Citation: Kondo, H.X.; Takano, Y. Conformational Preference of Flavonols and Its Effect on the Chemical Properties Involved in Radical Scavenging Activity. *Chemistry* **2022**, *4*, 1123–1135. https://doi.org/10.3390/chemistry4040076

Academic Editor: Maxim L. Kuznetsov

Received: 26 August 2022
Accepted: 20 September 2022
Published: 22 September 2022

1. Introduction

Free radicals, which contain unpaired electrons, are highly reactive and can trigger radical-chain reactions. In living systems, the concentration of free radicals is balanced by their production and removal and is maintained at a low level. Although free radicals are pivotal to human health [1–4], they damage several cellular components and are hazardous to living organisms at high concentrations [5,6].

Oxidative stress (OS) is a phenomenon in which an increase in the steady-state level of free radicals (or other highly reactive species) disturbs cellular processes and signaling pathways, leading to the oxidative modification of cellular components and, at worst, cell death [5]. OS often causes oxidative damage to vital biological molecules, such as proteins, lipids, and DNA, resulting in various diseases, such as cancer [7], allergies [8], immune system dysfunction [9], and cardiovascular disease [10]. Compounds with radical-scavenging activity, referred to as antioxidants, are a group of molecules that can lower OS in different ways [11]. Some terminate chain reactions via direct interaction with free radicals, some prevent radical formation by indirect interaction with radicals [12], and others repair oxidatively damaged molecules mainly by supplying electrons [13] or hydrogen.

Some antioxidants are multifunctional compounds. Because antioxidants can inhibit the harmful effects of free radicals, they have attracted significant attention, and quantitative analysis of their radical scavenging activity is an important research area.

Several experimental assays are used to estimate radical scavenging activity. There are two main radical scavenging mechanisms: single-electron transfer (SET) and hydrogen atom transfer (HAT). Antioxidant assays using DPPH (2,2-diphenyl-1-picrylhydrazyl) [14] and ABTS (3-ethylbenzothiazoline-6-sulfonic acid) [15] are based on SET or HAT [16,17]. Oxygen radical absorbance capacity (ORAC) [18] and total radical-trapping antioxidant parameter (TRAP) [19] assays, which mainly operate by HAT, are also widely used. The reactivity of a compound may change depending on the environment and reacting radicals. In particular, the polarity of the environment is an important factor in antioxidant activity. Therefore, antioxidant activity depends on the assay used. Frankel and Meyer [20] and Prior et al. [21] highlighted the great need for a standardized assay.

Recently, quantum chemistry-based methods have made significant contributions to chemical research [22]. Dramatic improvements in computational power and computer software have enabled us to calculate molecular properties related to radical scavenging activity with reliable accuracy and reasonable computational cost. Quantum chemical analysis has also been applied to the calculation of antioxidant activity, and a standardized analysis protocol has been proposed: quantum mechanics-based test for overall free radical scavenging activity (QM-ORSA) [11,23]. The QM-ORSA protocol considers all possible radical scavenging mechanisms, such as formal hydrogen transfer (FHT), which occurs by either HAT or proton-coupled electron transfer mechanisms (PCET), sequential proton loss electron transfer (SPLET), and single electron transfer followed by proton transfer (SET-PT), and discerns the main mechanism of antioxidant activity. A schematic representation of the radical scavenging mechanisms is presented in [17]. The QM-ORSA protocol was validated against experimental data [23–26] and successfully provided accurate radical scavenging activity. However, the problem with applying the QM-ORSA protocol is the large number of candidates for analysis (conformers and hydroxy groups).

This study focused on the challenges associated with applying the QM-ORSA protocol to flavonols. Flavonols (3-hydroxyflavones) are a class of flavonoids that have a 2-phenyl-4H-1-benzopyran-4-one skeleton [27] (Figure 1a), are found in various fruits and vegetables, and exhibit antioxidant activity [28,29]. Flavonoids, including flavonols, have two benzene rings called the A and B rings and a pyran ring called the C ring. In addition, flavonols possess a double bond between C2 and C3 and a carbonyl group at position 4 of the C ring, as shown in Figure 1. The chemical structure of flavonoids accommodates many conformations. We investigated the conformational dependence of the chemical properties of three types of flavonols with different numbers of hydroxy groups: myricetin, quercetin, and kaempferol (Figure 1b–d) [30]. Although the radical scavenging activity of these molecules has been previously investigated by DFT [29,31–33], their conformational dependence has not been discussed. To examine the possibility of narrowing down the candidates, we computed the bond dissociation energy (BDE) and ΔG^{o} of the reaction of the scavenger with $HOO^{\bullet}$, pK_a, and ionization energy (IE) for the O-H bond in each hydroxy group for several conformers of these three compounds, and showed the effect of the molecular conformation on these properties.

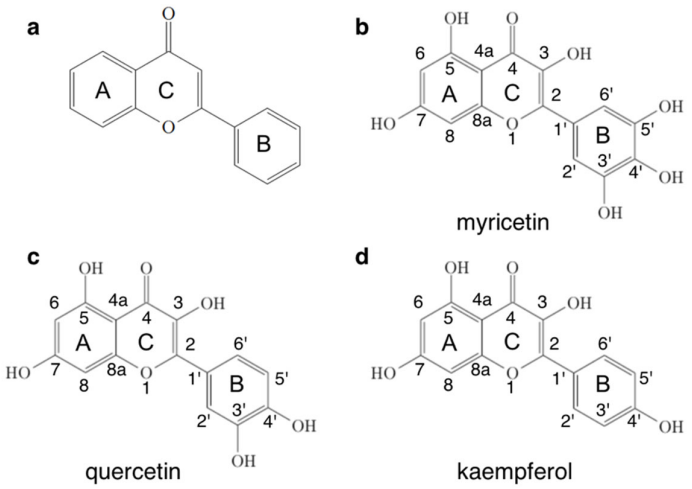

Figure 1. (**a**) Basic chemical structure of flavonol (2-phenyl-4H-1-benzopyran-4-one). Molecular structure of (**b**) myricetin, (**c**) quercetin, and (**d**) kaempferol. The A, B, and C rings and the numbering are shown.

2. Materials and Methods

2.1. DFT Calculation

All DFT calculations were performed using the Gaussian16 software [34]. We utilized the M06-2X/6-311++G(d,p) method [35,36] following the QM-ORSA protocol. The results were in agreement with the experimental results for both the thermodynamic and kinetic properties related to radical scavenging activity [24,37–40]. RODFT was used to compute the radicals.

2.2. Conformational Search in the Gas Phase or Aqueous Environment

The possible conformers were searched by using the Conflex software version 9 [41,42] with default parameters. All the obtained conformers were further optimized by DFT calculations in the gas phase and in water solvent. Thermal correction under standard conditions (298.15 K and 1.0 atm) was performed for the electronic energy of each optimized conformer to evaluate the enthalpies and Gibbs energies. Then, the probability of each conformer was calculated using the Gibbs energy according to the Boltzmann distribution law.

2.3. Calculation of the Bond Dissociation Energy (BDE)

To evaluate the likelihood of a reaction occurring by FHT, which includes HAT and PCET, for each bond, we calculated the BDE for each O-H bond. The BDE is calculated as follows:

$$\mathrm{BDE} = H(\mathrm{M}^{\bullet}) + H(\mathrm{H}^{\bullet}) - H(\mathrm{MH}), \quad (1)$$

where MH, M$^{\bullet}$, and H$^{\bullet}$ represent the neutral molecules of the scavengers, radical of scavengers, and hydrogen radicals, respectively, and $H(\bullet)$ is the enthalpy of each substance.

We also computed the ΔG^{o} for the radical scavenging reaction of HOO$^{\bullet}$ as Equation (2):

$$\mathrm{MH} + \mathrm{HOO}^{\bullet} \rightarrow \mathrm{M}^{\bullet} + \mathrm{HOOH}, \quad (2)$$

$$\Delta G^{o} = G^{o}(\mathrm{M}^{\bullet}) + G^{o}(\mathrm{HOOH}) - G^{o}(\mathrm{MH}) - G^{o}(\mathrm{HOO}^{\bullet}). \quad (3)$$

2.4. Computation of pKa

The acid dissociation constant (pK_a) of each molecule was evaluated to identify the possible radical scavenging mechanism. For the flavonols targeted in this study, we considered only the deprotonation of the hydroxy groups, as shown in Equation (4):

$$\mathrm{ROH} \rightleftharpoons \mathrm{RO^-} + \mathrm{H^+}. \quad (4)$$

Many theoretical pK_a calculations have been reported. In this study, the pK_a was calculated with the fitting parameter method [43] using experimental pKa data and the calculated Gibbs energy difference, based on Equation (4):

$$\mathrm{p}K_\mathrm{a} = m\Delta G^\mathrm{o} + C_0 \quad (5)$$

$$\Delta G^\mathrm{o} = G^\mathrm{o}_{\mathrm{A}^-} - G^\mathrm{o}_{\mathrm{HA}} \quad (6)$$

where ΔG^o is the Gibbs energy difference for deprotonation based on Equation (4), and m and C_0 are the fitted parameters. These fitted parameters were provided for several combinations of the DFT method and basis set in a previous study [44]. In this study, we set m to 0.318 and C_0 to −82.349 (fitted for M06-2X/6-311++G(d,p)). $G^\mathrm{o}_{\mathrm{A}^-}$ and $G^\mathrm{o}_{\mathrm{HA}}$ were calculated after geometry optimization, which was performed in solution using a solvation model based on density (SMD) [45].

2.5. Computation of IE

The ionization energy (IE) was computed to estimate the antioxidant activity through the SET mechanism, together with the first step of SET-PT or the second step of SPLET. The BDE was calculated as follows:

$$\mathrm{IE} = H(\mathrm{MH^{+\bullet}}) + H(\mathrm{e^-}) - H(\mathrm{MH}), \quad (7)$$

where $\mathrm{MH^{+\bullet}}$ is the radical cation of the scavenger. The value of $H(\mathrm{e^-})$ in water was obtained from literature [46].

3. Results and Discussion

3.1. Conformational Search of Each Flavonol Molecule in the Gas Phase

The conformational search via Conflex software revealed 25, 23, and 15 conformers for myricetin, quercetin, and kaempferol, respectively. Our computational results showed that the main conformational differences between the obtained conformers were the rotation around the C2-C1′ bond and the orientation of the hydrogen atom of the hydroxy groups. Geometry optimizations and frequency calculations were performed for all conformers at the M06-2X/6-311++G(d,p) level of theory in the gas phase. The Gibbs energy of each conformer was also computed. The calculated Gibbs energies and dihedral angles of C3-C2-C1′-C2′ in the optimized conformation are shown in Table S1. Hereafter, we refer to the dihedral angle of atoms A, B, C, and D as $\omega_{\text{A-B-C-D}}$. For myricetin and kaempferol, the structures with $\omega_{\text{C3-C2-C1′-C2′}} = 0°$ and $\omega_{\text{C3-C2-C1′-C2′}} = 180°$ are identical because the symmetry of the B ring. For all three molecules, three stable regions existed for rotation around the C2-C1′ bond: $\omega_{\text{C3-C2-C1′-C2′}} = \sim 0°$, ±~10°, and ±~40° for myricetin and kaempferol, and ~0°, ~140°, and ±~170° for quercetin. The planar structure was most stable in myricetin ($\omega_{\text{C3-C2-C1′-C2′}} = 0.1°$) and quercetin ($\omega_{\text{C3-C2-C1′-C2′}} = -1.2°$), and conformers with slightly twisted structures were also stable in quercetin ($\omega_{\text{C3-C2-C1′-C2′}} = 171.8°$) and kaempferol ($\omega_{\text{C3-C2-C1′-C2′}} = 9.4°$, −10.9°, 13.2°, and 13.9°). For myricetin, a difference in energy with respect to $\omega_{\text{C3-C2-C1′-C2′}}$ was reported [31]. Our results agree that the planar structure is the most stable, but not in the other conformers. This is because we also considered the orientation of the hydrogen atoms of the hydroxy groups in addition to the rotation around the C2-C1′ bond.

Conformer pairs with a difference in the Gibbs energy ≤ 0.00002 Hartree and with the same orientation of the hydrogen atom of hydroxy groups were regarded as identical (axial chirality was included), and only one of the identical conformers was retained. At this stage, 18, 17, and 12 conformers remained for myricetin, quercetin, and kaempferol,

respectively. We then computed the relative population from the Gibbs energy of each conformer and excluded conformers with a relative population of <1%. This left four, six, and four conformers for myricetin, quercetin, and kaempferol, respectively (Table 1 and Figure 2). The conformer indices are provided in descending order of relative population of each molecule. We used these conformer indices in gas-phase analyses. The atomic coordinates of each conformer are shown in the SI.

Table 1. Relative population (probability) and dihedral angles of C3-C2-C1′-C2′ after the geometry optimization with DFT for each conformer. The values of $\omega_{C3\text{-}C2\text{-}C1'\text{-}C2'}$ are shown in degrees.

	Myricetin		Quercetin		Kaempferol	
Conf. Index	**Probability**	$\omega_{C3\text{-}C2\text{-}C1'\text{-}C2'}$	**Probability**	$\omega_{C3\text{-}C2\text{-}C1'\text{-}C2'}$	**Probability**	$\omega_{C3\text{-}C2\text{-}C1'\text{-}C2'}$
g-1	0.534	0.1	0.475	−1.2	0.385	9.4
g-2	0.354	0.0	0.257	−3.8	0.310	−10.9
g-3	0.075	11.1	0.143	4.9	0.161	13.9
g-4	0.035	−13.3	0.082	171.8	0.144	13.2
g-5	-	-	0.023	168.1	-	-
g-6	-	-	0.019	167.6	-	-

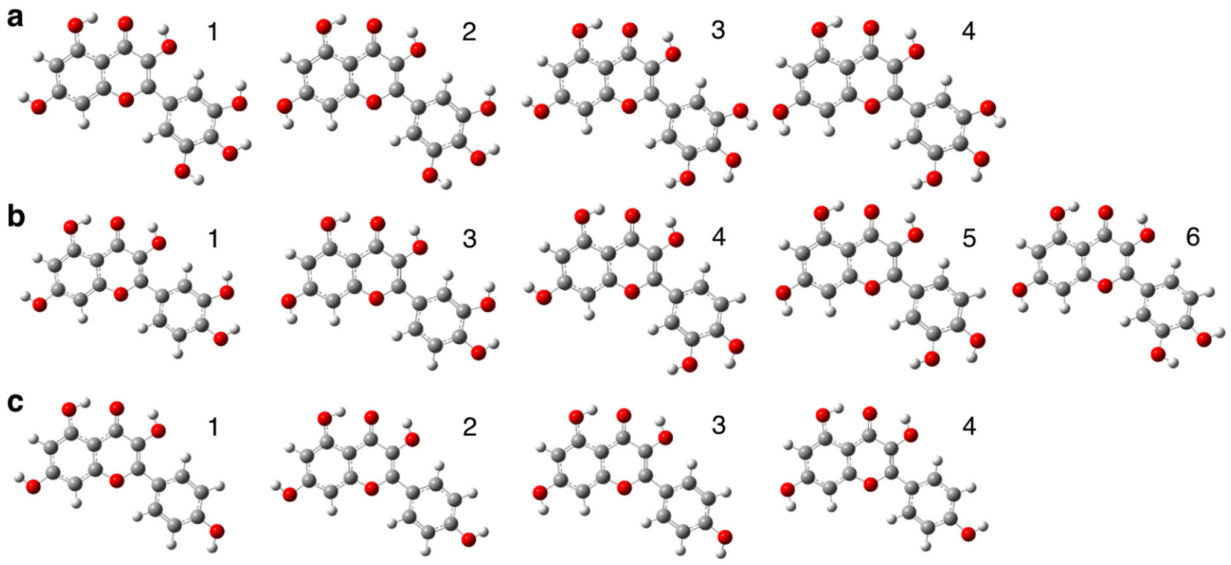

Figure 2. Conformers obtained by geometry optimization with DFT in the gas phase for (**a**) myricetin, (**b**) quercetin, and (**c**) kaempferol. Numbers in the upper right for each molecule represent their conformer indices. For quercetin, conformer 2 is omitted because the orientation of the hydrogen atom in the hydroxy groups of the conformer 2 is the same as that of conformer 1.

We classified the conformation of each molecule by rotation around the C2-C1′ bond, $\omega_{C3\text{-}C2\text{-}C1'\text{-}C2'}$, and orientation of the hydrogen atom of the hydroxy groups. We refer to the dihedral angles representing the orientation of the hydrogen atoms as A_1, A_2, B_1, B_2, B_3, and C, as shown in Figure 3. Each orientation can be classified into two or three patterns, as listed in Table 2. For "A_1 and C," the absolute value of dihedral angle of 155.0° ≤ C ≤ 180.0° was included in case II. For others, a deviation of ±5° was allowed.

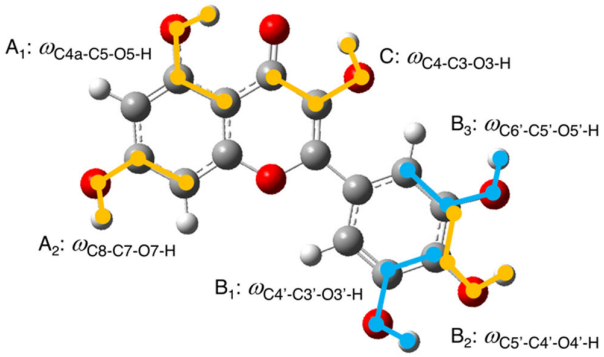

Figure 3. Definition of the dihedral angles representing the orientation of hydrogen atoms of each hydroxy group. The four atoms constituting a dihedral angle are represented using orange and blue balls and lines.

Table 2. The combinations of the orientation of hydrogen atoms in each hydroxy group.

Molecule	A_1 and C	A_2	B_1, B_2, and B_3
myricetin	I.$A_1 \approx 0°$ and $C \approx 0°$ II.($A_1 \approx 180°$ and $C \approx 0°$) or ($A_1 \approx 0°$ and $C \approx 180°$)	I. $A_2 \approx 0°$ II. $A_2 \approx 180°$	I.$B_1 \approx 0°$ and $B_2 \approx 0°$ and $B_3 \approx 0°$ II.$B_1 \approx 180°$ and $B_2 \approx 180°$ and $B_3 \approx 180°$ III.others
quercetin	I.$A_1 \approx 0°$ and $C \approx 0°$ II.($A_1 \approx 180°$ and $C \approx 0°$) or ($A_1 \approx 0°$ and $C \approx 180°$)	I. $A_2 \approx 0°$ II. $A_2 \approx 180°$	I.$B_1 \approx 0°$ and $B_2 \approx 0°$ II.$B_1 \approx 180°$ and $B_2 \approx 180°$
kaempferol	I.$A_1 \approx 0°$ and $C \approx 0°$ II.($A_1 \approx 180°$ and $C \approx 0°$) or ($A_1 \approx 0°$ and $C \approx 180°$)	I. $A_2 \approx 0°$ II. $A_2 \approx 180°$	I.$B_2 \approx 0°$ II.$B_2 \approx 180°$

We found that (1) the conformers with pattern I for "A_1 and C" in Table 2 were significantly more stable than those with pattern II, (2) the conformers with pattern III for "B_1, B_2, and B_3" show a significantly higher electronic energy than those with cases I or II, and (3) the dihedral angle A_2 does not substantially affect electronic energy. Even some conformers in pattern III for "B_1, B_2, and B_3" as the initial structures resulted in conformations with pattern I or II after geometry optimization via DFT calculations. All conformers in Table 1 were classified into pattern I of "A_1 and C" and pattern I or II for "B_1, B_2, and B_3." This is because the hydrogen bonds between the hydroxy groups and the ketone group at position 4 for the orientations of A_1 and C, and the hydrogen bonds between the hydroxy groups and the π-conjugation of the phenyl ring with the hydroxy groups for the orientations of B_1, B_2, and B_3 stabilize the conformation. In kaempferol, the dihedral angle B_2 does not significantly affect electronic energy because there is only one hydroxy group in the B ring. In addition, in the pattern of $C \approx 180°$, the B ring has to rotate around the C2-C1′ bond at ~40° to prevent any steric hindrance, for example, conformers of myricetin with indices x, xi, and xii and those of kaempferol with indices v, vi, and vii. Such rotation of the B ring may decrease the conformational stability of these conformers.

3.2. Conformational Search of Each Flavonol Molecule in the Aqueous Environment

We also carried out a conformational search in water on the same conformers as in Section 3.1, to determine whether it could substitute that in the gas phase. The initial structures for geometry optimization were the same as those used in Section 3.1. The calculated Gibbs energies and dihedral angles $\omega_{C3\text{-}C2\text{-}C1'\text{-}C2'}$ for each optimized structure are listed in Table S2. Identical and major conformers were selected using the method described in

Section 3.1, and their relative populations were calculated (Table 3). The conformer indices were provided in descending order of relative population and were used in subsequent aqueous solution analyses. The atomic coordinates of each conformer are included in the SI.

Table 3. The relative population (probability) and dihedral angles of C3-C2-C1′-C2′ after the geometry optimization using DFT for each conformer. Values of $\omega_{C3\text{-}C2\text{-}C1'\text{-}C2'}$ are shown in degrees.

	Myricetin		Quercetin		Kaempferol	
Conf. Index	**Probability**	$\omega_{C3\text{-}C2\text{-}C1'\text{-}C2'}$	**Probability**	$\omega_{C3\text{-}C2\text{-}C1'\text{-}C2'}$	**Probability**	$\omega_{C3\text{-}C2\text{-}C1'\text{-}C2'}$
w-1	0.368 (g-2) †	27.0	0.390 (g-2)	−27.8	0.295 (g-2)	−29.5
w-2	0.181 (g-4)	−25.4	0.183 (g-3)	26.6	0.290 (g-1)	31.0
w-3	0.165 (g-1)	27.0	0.108 (g-6)	151.5	0.209 (g-3)	30.6
w-4	0.125 (none)	25.4	0.103 (g-5)	152.8	0.192 (g-4)	29.9
w-5	0.094 (g-3)	26.6	0.087 (g-4)	153.5	-	-
w-6	0.052 (none)	25.7	0.043 (none)	152.3	-	-
w-7	-	-	0.037 (none)	153.0	-	-
w-8	-	-	0.035 (none)	27.4	-	-

† Values in the parentheses represent the conformer indices in the gas phase.

The stable regions for rotation around the C2-C1′ bond in an aqueous environment were different from those in the gas phase. While the molecules prefer $\omega_{C3\text{-}C2\text{-}C1'\text{-}C2'}$ = ~0° or ± ~10° in the gas phase, they favor a more twisted structure; $\omega_{C3\text{-}C2\text{-}C1'\text{-}C2'}$ = ±~30°, or ±~40° in aqueous environments. In a previous study, quercetin was predicted to be planar [33]. This may be caused by the difference in conformational sampling of the orientation of the hydrogen atoms of the hydroxy groups. Although the major conformers were the same as those in the gas phase, the order of the relative population differed from that calculated in the gas phase, suggesting the necessity for a separate conformational search in water. Among the tendencies described in Section 3.1, the major difference in the conformational search in water was that the conformers with pattern III for "B_1, B_2, and B_3" have probabilities of more than 1% and were found in Table 3, which may be attributed to a weaker electrostatic repulsion in water than that in the gas phase due to the high dielectricity of water. For "A_1 and C," case I was the only analysis target, as in the gas phase.

3.3. BDE and ΔG^o of the Reaction of Scavenger with HOO• for O-H Bond in Each Hydroxy Group

The calculated BDE and ΔG^o values are presented in Table 4. Because the most stable conformation is the one in which the hydrogen atoms of the hydroxy groups adjacent to the radicalized hydroxy group are in proximity to the radicalized hydroxy group, the orientation of the hydrogen atom(s) was changed before geometry optimization of the radicalized molecules (Figure S1).

Table 4. BDE and ΔG^o of the reaction of the scavenger with the HOO• for O-H bond in each hydroxy group.

Conf. Index/Position	Myricetin	Quercetin	Kaempferol
	BDE (ΔG^o) †	**BDE (ΔG^o)**	**BDE (ΔG^o)**
g-1/O3	86.7 (8.1) ‡	86.4 (8.0)	87.2 (8.1)
g-2/O3	87.1 (8.4)	86.4 (7.6)	87.0 (7.7)
g-3/O3	87.7 (8.0)	86.7 (7.8)	87.5 (8.1)
g-4/O3	88.0 (8.4)	87.1 (7.9)	87.3 (7.8)
g-5/O3	-	87.3 (7.7)	-
g-6/O3	-	87.5 (8.1)	-
mean of ΔG^o	8.2 ± 0.2	7.8 ± 0.2	7.9 ± 0.2

g-1/O5	103.5 (24.1)	103.6 (24.0)	103.8 (24.0)
g-2/O5	104.4 (24.9)	103.6 (23.6)	103.6 (23.7)
g-3/O5	103.9 (24.0)	104.5 (24.7)	104.6 (24.7)
g-4/O5	103.9 (25.8)	104.0 (24.3)	104.6 (24.7)
g-5/O5	-	104.0 (25.9)	-
g-6/O5	-	103.8 (25.7)	-
mean of ΔG^{o}	24.7 ± 0.7	24.7 ± 0.8	24.3 ± 0.4
g-1/O7	96.6 (17.1)	95.9 (19.5)	96.4 (17.3)
g-2/O7	96.4 (16.8)	96.5 (17.4)	96.4 (17.3)
g-3/O7	96.5 (17.4)	96.2 (17.1)	95.9 (16.7)
g-4/O7	95.8 (16.9)	96.3 (16.6)	96.0 (16.8)
g-5/O7	-	95.7 (15.9)	-
g-6/O7	-	96.2 (17.0)	-
mean of ΔG^{o}	17.1 ± 0.2	17.2 ± 1.1	17.0 ± 0.2
g-1/O3′	84.5 (8.4)	84.0 (6.5)	-
g-2/O3′	84.6 (8.6)	83.9 (6.0)	-
g-3/O3′	84.5 (6.1)	84.1 (6.2)	-
g-4/O3′	84.1 (5.8)	83.1 (5.0)	-
g-5/O3′	-	82.7 (4.5)	-
g-6/O3′		82.8 (4.4)	
mean of ΔG^{o}	7.2 ± 1.3	5.4 ± 0.8	-
g-1/O4′	76.2 (0.4)	81.8 (3.2)	89.8 (10.2)
g-2/O4′	76.2 (0.5)	81.7 (2.7)	89.9 (10.0)
g-3/O4′	75.5 (−0.7)	81.2 (5.1)	89.7 (9.6)
g-4/O4′	75.7 (−2.7)	81.2 (2.4)	89.9 (9.4)
g-5/O4′	-	80.9 (1.9)	90.3 (8.7)
g-6/O4′	-	81.1 (1.8)	
mean of ΔG^{o}	−0.6 ± 1.3	2.9 ± 1.1	9.8 ± 0.3
g-1/O5′	84.6 (8.6)	-	-
g-2/O5′	84.8 (8.8)	-	-
g-3/O5′	84.5 (6.0)	-	-
g-4/O5′	84.2 (5.9)	-	-
g-5/O5′	-	-	-
g-6/O5′	-	-	-
mean of ΔG^{o}	7.3 ± 1.4	-	-

† BDE and ΔG^{o} are expressed in kcal/mol. ‡ Values in the parentheses represent ΔG^{o}.

The standard deviations of ΔG^{o} (Table 4) were less than 1.0 kcal/mol at most positions, indicating that ΔG^{o} (or BDE) is not sensitive to structural differences. The BDE values for the hydroxy groups of the A and C rings were nearly equal for the three molecules, suggesting that the chemical structure of the B ring had a negligible effect on the BDE of the hydroxy groups of the A and C rings. Bond dissociation was the most probable at the hydroxy group at position 4′ for myricetin and quercetin, and ΔG^{o} for myricetin was smaller than that for quercetin. This is because the formation of the hydrogen bonds stabilizes the conformation. The hydroxy group at position 4′ of myricetin provided the smallest ΔG^{o} because the radical could be stabilized via hydrogen bonding with the two hydroxy groups at positions 3′ and 5′. The calculated ΔG^{o} values indicated that HAT could spontaneously occur only at the O4′–H bond of myricetin. For kaempferol, bond dissociation was most likely to occur at the hydroxy group of position 3, but the Gibbs energy for bond dissociation was high; the mean value over four conformers was 7.9 kcal/mol, suggesting that radical scavenging via the FHT mechanism does not occur in the gas phase.

3.4. Calculated pKa for Each Hydroxy Group

We estimated pK_a using Equations (5) and (6), as described in Section 2.4. The calculated pK_a values for each position are listed in Table 5. As described in Section 3.3, the orientation of the hydrogen atom(s) was changed before geometry optimization of the ionized molecules, as shown in Figure S1, because the modified conformation is more energetically stable than the original one. The standard deviation of the pK_a below 0.2 for all positions implies that the pK_a value is not sensitive to structural differences.

Myricetin deprotonates at the position 4′ hydroxy group and the other two molecules deprotonate at the position 7 hydroxy group at physiological pH (pH = 7.4). For the B ring, the proton bound to the hydroxy group at position 4′ was the most likely to dissociate. This observation corresponds to the results of a previous study by Fiorucci et al. [33]. The order of probable ionization was myricetin, quercetin, and kaempferol, descending. This is because hydrogen bond formation contributes to conformation stability. Similar to BDE, for the A and C rings, the pK_a values of the hydroxy groups at the three positions (3, 5, and 7) of all three molecules were nearly equal, indicating that the pK_a values of the hydroxy groups in the A and C rings were not affected by the chemical structure of the B ring. This is because the additional charge by deprotonation is distributed only on the A ring upon the ionization of the hydroxy group at positions 3, 5, and 7 [33].

Table 5. Calculated pK_a for the O-H bond in each hydroxy group.

Conf. Index/Position	Myricetin	Quercetin	Kaempferol
w-1/O3	8.1	8.6	8.6
w-2/O3	8.4	8.5	8.6
w-3/O3	8.2	8.4	8.6
w-4/O3	8.5	8.4	8.6
w-5/O3	8.2	8.4	-
w-6/O3	8.3	8.5	-
w-7/O3	-	8.5	-
w-8/O3	-	8.4	-
mean	8.3 ± 0.1	8.5 ± 0.1	8.6 ± 0.0
w-1/O5	8.7	8.6	8.7
w-2/O5	8.8	8.6	8.7
w-3/O5	9.0	8.7	8.7
w-4/O5	8.7	8.6	8.7
w-5/O5	8.6	8.5	-
w-6/O5	8.5	8.7	-
w-7/O5	-	8.6	-
w-8/O5	-	8.5	-
mean	8.7 ± 0.2	8.6 ± 0.1	8.7 ± 0.0
w-1/O7	7.5	7.5	7.4
w-2/O7	7.5	7.4	7.5
w-3/O7	7.3	7.4	7.4
w-4/O7	7.5	7.5	7.4
w-5/O7	7.4	7.4	-
w-6/O7	7.3	7.4	-
w-7/O7	7.5	7.4	-
w-8/O7	7.5	7.5	-
mean	7.4 ± 0.1	7.4 ± 0.0	7.4 ± 0.0
w-1/O3′	8.2	8.4	-
w-2/O3′	8.1	8.3	-
w-3/O3′	8.2	8.1	-

w-4/O3′	8.0	8.1	-
w-5/O3′	8.1	8.2	-
w-6/O3′	8.0	8.0	-
w-7/O3′	-	8.0	-
w-8/O3′	-	7.9	-
mean	8.1 ± 0.1	8.1 ± 0.1	
w-1/O4′	6.8	7.6	8.4
w-2/O4′	6.7	7.6	8.4
w-3/O4′	6.7	7.4	8.5
w-4/O4′	6.6	7.4	8.4
w-5/O4′	6.6	7.5	-
w-6/O4′	6.4	7.3	-
w-7/O4′	-	7.3	-
w-8/O4′	-	7.2	-
mean	6.6 ± 0.1	7.4 ± 0.1	8.4 ± 0.0
w-1/O5′	8.2	-	-
w-2/O5′	8.0	-	-
w-3/O5′	8.1	-	-
w-4/O5′	7.9	-	-
w-5/O5′	8.0	-	-
w-6/O5′	7.9	-	-
w-7/O5′	-	-	-
w-8/O5′	-	-	-
mean	8.0 ± 0.1		

3.5. Calculated IE in the Aqueous Environment

The IE of each conformer for each molecule in water was calculated (Table 6). The standard deviations of the IEs were within 0.4 kcal/mol for all three molecules, implying that IE, similar to BDE and pK_a, is not influenced by conformational differences. All molecules exhibited nearly equal IE values. The previous study also yielded nearly identical IE values for myricetin and quercetin, though those of kaempferol were slightly larger [32]. The dihedral angle $\omega_{C3\text{-}C2\text{-}C1'\text{-}C2'}$ changed slightly upon ionization and radicalization, whereas the neutral molecule preferred $\omega_{C3\text{-}C2\text{-}C1'\text{-}C2'}$ = ± ~30° (or ~150° for quercetin), the radical cation preferred a more planar structure, $\omega_{C3\text{-}C2\text{-}C1'\text{-}C2'}$ = ± ~10° (or ~165° for quercetin; Table S3).

Table 6. The calculated IEs for each conformer and the means and standard deviations of the IEs for each molecule (kcal/mol).

Conf. Index	Myricetin	Quercetin	Kaempferol
w-1	111.93	111.72	111.15
w-2	111.75	111.45	111.44
w-3	111.13	111.60	111.55
w-4	111.78	111.65	111.50
w-5	111.63	111.41	-
w-6	110.97	111.55	-
w-7	-	111.48	-
w-8	-	111.44	-
mean	111.5 ± 0.4	111.5 ± 0.1	111.2 ± 0.4

4. Conclusions

In this study, we investigated the effect of conformational differences on three chemical properties involved in the radical scavenging activity—BDE, pK_a, and IE—for three flavonols: myricetin, quercetin, and kaempferol. A conformational search was first performed for each molecule in the gas and aqueous phases. We observed the following commonalities among stable conformers: (1) the conformers with pattern I for the dihedral angles A_1 and C (Table 2) and (2) the conformers with pattern I or II in the gas phase. In an aqueous environment, conformers with pattern III for "B_1, B_2, and B_3" are also probable. Although a planar structure was used for myricetin and quercetin in the previous studies, we found that the conformers twisted around the C2-C1′ bond are more stable in the aqueous environments. Because the stable conformation and relative population in the gas phase were different from those in the aqueous solution, a separate conformational search is required for these phases.

The calculations of BDE, pK_a, and IE showed that these chemical properties were uninfluenced by structural differences among the conformers. Therefore, we surmise that it is better to select the conformer with the lowest conformational energy to analyze the chemical properties. The BDE and pK_a values of the hydroxy groups at the three positions (3, 5, and 7) of rings A and C of all three molecules were not affected by the chemical structure of ring B. The Gibbs energies of bond dissociation indicate that radical scavenging via the FHT mechanism in the gas phase is only possible for myricetin. The pK_a value of each hydroxy group indicates that these three molecules can function as radical scavengers in aqueous environments. For myricetin, the hydroxy group at position 4′ is most likely to be deprotonated, and the other two molecules deprotonate at the position 7 hydroxy group at physiological pH. In the future studies, we will attempt to investigate the effect of the conformational differences on the kinetic properties of the radical scavenging activity.

Supplementary Materials: The following supporting information can be downloaded at: www.mdpi.com/article/10.3390/chemistry4040076/s1, Figure S1: Change in the orientation of hydrogen atoms upon radicalization or ionization; Table S1: Gibbs energies and dihedral angles of C3-C2-C1′-C2′ after the geometry optimization using DFT in the gas phase; Table S2: Gibbs energies and dihedral angles of C3-C2-C1′-C2′ after the geometry optimization using DFT in water; Table S3: Dihedral angles of C3-C2-C1′-C2′ in the neutral molecule and radical cation.

Author Contributions: Conceptualization, H.X.K. and Y.T.; methodology, H.X.K. and Y.T.; software, H.X.K. and Y.T.; validation, H.X.K. and Y.T.; formal analysis, H.X.K. and Y.T.; investigation, H.X.K. and Y.T.; resources, H.X.K. and Y.T.; data curation, H.X.K. and Y.T.; writing—original draft preparation, H.X.K. and Y.T.; writing—review and editing, H.X.K. and Y.T.; visualization, H.X.K.; supervision, Y.T.; project administration, H.X.K. and Y.T.; funding acquisition, H.X.K. and Y.T. Both authors have read and agreed to the published version of the manuscript.

Funding: This research was funded by FY 2022 President's Discretionary Grants, Kitami Institute of Technology. We are grateful to the Ministry of Education, Culture, Sports, Science, and Technology (MEXT) for a Grant-in-Aid for Scientific Research on Transformative Research Areas (A) "Hyper-Ordered Structures Science," 20H05883, and to the Japan Society for the Promotion of Science (JSPS), 19K06589, 19H02752, and 22K06164.

Data Availability Statement: Not applicable.

Acknowledgments: The computations were performed at the Research Center for Computational Science, Okazaki, Japan (22-IMS-C007), and the RIKEN Advanced Center for Computing and Communication (ACCC). This study was performed in part under the Cooperative Research Program of the Institute for Protein Research, Osaka University, CR-22-02.

Conflicts of Interest: The authors declare no conflict of interest.

References

1. Dröge, W. Free Radicals in the Physiological Control of Cell Function. *Physiol. Rev.* **2002**, *82*, 47–95. https://doi.org/10.1152/physrev.00018.2001.

2. Halliwell, B. Biochemistry of Oxidative Stress. *Biochem. Soc. Trans.* **2007**, *35*, 1147–1150. https://doi.org/10.1042/BST0351147.
3. Pacher, P.; Beckman, J.S.; Liaudet, L. Nitric Oxide and Peroxynitrite in Health and Disease. *Physiol. Rev.* **2007**, *87*, 315–424. https://doi.org/10.1152/physrev.00029.2006.
4. Genestra, M. Oxyl Radicals, Redox-Sensitive Signalling Cascades and Antioxidants. *Cell. Signal.* **2007**, *19*, 1807–1819. https://doi.org/10.1016/j.cellsig.2007.04.009.
5. Lushchak, V.I. Free Radicals, Reactive Oxygen Species, Oxidative Stresses and Their Classifications. *Ukr. Biochem. J.* **2015**, *87*, 11–18. https://doi.org/10.15407/ubj87.06.011.
6. Riley, P.A. Free Radicals in Biology: Oxidative Stress and the Effects of Ionizing Radiation. *Int. J. Radiat. Biol.* **1994**, *65*, 27–33. https://doi.org/10.1080/09553009414550041.
7. Sainz, R.M.; Lombo, F.; Mayo, J.C. Radical Decisions in Cancer: Redox Control of Cell Growth and Death. *Cancers* **2012**, *4*, 442–474. https://doi.org/10.3390/cancers4020442.
8. Dozor, A.J. The Role of Oxidative Stress in the Pathogenesis and Treatment of Asthma. *Ann. N. Y. Acad. Sci.* **2010**, *1203*, 133–137. https://doi.org/10.1111/j.1749-6632.2010.05562.x.
9. Zhou, R.; Tardivel, A.; Thorens, B.; Choi, I.; Tschopp, J. Thioredoxin-Interacting Protein Links Oxidative Stress to Inflammasome Activation. *Nat. Immunol.* **2010**, *11*, 136–140. https://doi.org/10.1038/ni.1831.
10. Rochette, L.; Lorin, J.; Zeller, M.; Guilland, J.-C.; Lorgis, L.; Cottin, Y.; Vergely, C. Nitric Oxide Synthase Inhibition and Oxidative Stress in Cardiovascular Diseases: Possible Therapeutic Targets? *Pharmacol. Ther.* **2013**, *140*, 239–257. https://doi.org/10.1016/j.pharmthera.2013.07.004.
11. Galano, A.; Raúl Alvarez-Idaboy, J. Computational Strategies for Predicting Free Radical Scavengers' Protection against Oxidative Stress: Where Are We and What Might Follow? *Int. J. Quantum Chem.* **2019**, *119*, e25665. https://doi.org/10.1002/qua.25665.
12. Kumar, N.; Goel, N. Phenolic Acids: Natural Versatile Molecules with Promising Therapeutic Applications. *Biotechnol. Rep.* **2019**, *24*, e00370. https://doi.org/10.1016/j.btre.2019.e00370.
13. Pham-Huy, L.A.; He, H.; Pham-Huy, C. Free Radicals, Antioxidants in Disease and Health. *Int. J. Biomed. Sci.* **2008**, *4*, 89–96.
14. Sanchez-Moreno, C. Review: Methods Used to Evaluate the Free Radical Scavenging Activity in Foods and Biological Systems. *Food Sci. Technol. Int.* **2002**, *8*, 121–137. https://doi.org/10.1106/108201302026770.
15. Re, R.; Pellegrini, N.; Proteggente, A.; Pannala, A.; Yang, M.; Rice-Evans, C. Antioxidant Activity Applying an Improved ABTS Radical Cation Decolorization Assay. *Free Radic. Biol. Med.* **1999**, *26*, 1231–1237. https://doi.org/10.1016/S0891-5849(98)00315-3.
16. Goupy, P.; Dufour, C.; Loonis, M.; Dangles, O. Quantitative Kinetic Analysis of Hydrogen Transfer Reactions from Dietary Polyphenols to the DPPH Radical. *J. Agric. Food Chem.* **2003**, *51*, 615–622. https://doi.org/10.1021/jf025938l.
17. Platzer, M.; Kiese, S.; Herfellner, T.; Schweiggert-Weisz, U.; Miesbauer, O.; Eisner, P. Common Trends and Differences in Antioxidant Activity Analysis of Phenolic Substances Using Single Electron Transfer Based Assays. *Molecules* **2021**, *26*, 1244. https://doi.org/10.3390/molecules26051244.
18. Prior, R.L.; Cao, G. Analysis of Botanicals and Dietary Supplements for Antioxidant Capacity: A Review. *J. AOAC Int.* **2000**, *83*, 950–956. https://doi.org/10.1093/jaoac/83.4.950.
19. Evelson, P.; Travacio, M.; Repetto, M.; Escobar, J.; Llesuy, S.; Lissi, E.A. Evaluation of Total Reactive Antioxidant Potential (TRAP) of Tissue Homogenates and Their Cytosols. *Arch. Biochem. Biophys.* **2001**, *388*, 261–266. https://doi.org/10.1006/abbi.2001.2292.
20. Frankel, E.N.; Meyer, A.S. The Problems of Using One-Dimensional Methods to Evaluate Multifunctional Food and Biological Antioxidants. *J. Sci. Food Agric.* **2000**, *80*, 1925–1941. https://doi.org/10.1002/1097-0010(200010)80:13<1925::AID-JSFA714>3.0.CO;2-4.
21. Prior, R.L.; Wu, X.; Schaich, K. Standardized Methods for the Determination of Antioxidant Capacity and Phenolics in Foods and Dietary Supplements. *J. Agric. Food Chem.* **2005**, *53*, 4290–4302. https://doi.org/10.1021/jf0502698.
22. Spiegel, M. Current Trends in Computational Quantum Chemistry Studies on Antioxidant Radical Scavenging Activity. *J. Chem. Inf. Model.* **2022**, *62*, 2639–2658. https://doi.org/10.1021/acs.jcim.2c00104.
23. Galano, A.; Alvarez-Idaboy, J.R. A Computational Methodology for Accurate Predictions of Rate Constants in Solution: Application to the Assessment of Primary Antioxidant Activity. *J. Comput. Chem.* **2013**, *34*, 2430–2445. https://doi.org/10.1002/jcc.23409.
24. Dzib, E.; Cabellos, J.L.; Ortíz-Chi, F.; Pan, S.; Galano, A.; Merino, G. Eyringpy: A Program for Computing Rate Constants in the Gas Phase and in Solution. *Int. J. Quantum Chem.* **2019**, *119*, e25686. https://doi.org/10.1002/qua.25686.
25. Alvarez-Idaboy, J.R.; Galano, A. On the Chemical Repair of DNA Radicals by Glutathione: Hydrogen vs Electron Transfer. *J. Phys. Chem. B* **2012**, *116*, 9316–9325. https://doi.org/10.1021/jp303116n.
26. Vo, Q.V.; Bay, M. Van; Nam, P.C.; Mechler, A. Is Indolinonic Hydroxylamine a Promising Artificial Antioxidant? *J. Phys. Chem. B* **2019**, *123*, 7777–7784. https://doi.org/10.1021/acs.jpcb.9b05160.
27. Rauter, A.P.; Ennis, M.; Hellwich, K.-H.; Herold, B.J.; Horton, D.; Moss, G.P.; Schomburg, I. Nomenclature of Flavonoids (IUPAC Recommendations 2017). *Pure Appl. Chem.* **2018**, *90*, 1429–1486. https://doi.org/10.1515/pac-2013-0919.
28. Ma, Y.; Feng, Y.; Diao, T.; Zeng, W.; Zuo, Y. Experimental and Theoretical Study on Antioxidant Activity of the Four Anthocyanins. *J. Mol. Struct.* **2020**, *1204*, 127509. https://doi.org/10.1016/j.molstruc.2019.127509.
29. Spiegel, M.; Andruniów, T.; Sroka, Z. Flavones' and Flavonols' Antiradical Structure–Activity Relationship—A Quantum Chemical Study. *Antioxidants* **2020**, *9*, 461. https://doi.org/10.3390/antiox9060461.

30. Rice-Evans, C.A.; Miller, N.J.; Paganga, G. Structure-Antioxidant Activity Relationships of Flavonoids and Phenolic Acids. *Free Radic. Biol. Med.* **1996**, *20*, 933–956. https://doi.org/10.1016/0891-5849(95)02227-9.
31. Xie, H.J.; Mou, W.S.; Lin, F.R.; Xu, J.H.; Lei, Q.F. Radical Scavenging Activity of Myricetin. *Acta Physico-Chimica Sin.* **2013**, *29*, 1421–1432. https://doi.org/10.3866/PKU.WHXB201304222.
32. Nakanishi, I.; Ohkubo, K.; Shoji, Y.; Fujitaka, Y.; Shimoda, K.; Matsumoto, K.; Fukuhara, K.; Hamada, H. Relationship between the Radical-Scavenging Activity of Selected Flavonols and Thermodynamic Parameters Calculated by Density Functional Theory. *Free Radic. Res.* **2020**, *54*, 535–539. https://doi.org/10.1080/10715762.2020.1813887.
33. Fiorucci, S.; Golebiowski, J.; Cabrol-Bass, D.; Antonczak, S. DFT Study of Quercetin Activated Forms Involved in Antiradical, Antioxidant, and Prooxidant Biological Processes. *J. Agric. Food Chem.* **2007**, *55*, 903–911. https://doi.org/10.1021/jf061864s.
34. Frisch, M.J.; Trucks, G.W.; Schlegel, H.B.; Scuseria, G.E.; Robb, M.A.; Cheeseman, J.R.; Scalmani, G.; Barone, V.; Petersson, G.A.; Nakatsuji, H.; et al. *Gaussian 16, Revision C.01*; Gaussian, Inc.: Wallingford, CT, USA, 2016.
35. Zhao, Y.; Truhlar, D.G. The M06 Suite of Density Functionals for Main Group Thermochemistry, Thermochemical Kinetics, Noncovalent Interactions, Excited States, and Transition Elements: Two New Functionals and Systematic Testing of Four M06-Class Functionals and 12 Other Function. *Theor. Chem. Acc.* **2008**, *120*, 215–241. https://doi.org/10.1007/s00214-007-0310-x.
36. Cagnina, S.; Rotureau, P.; Fayet, G.; Adamo, C. The Ammonium Nitrate and Its Mechanism of Decomposition in the Gas Phase: A Theoretical Study and a DFT Benchmark. *Phys. Chem. Chem. Phys.* **2013**, *15*, 10849. https://doi.org/10.1039/c3cp50368b.
37. Zhao, Y.; Schultz, N.E.; Truhlar, D.G. Design of Density Functionals by Combining the Method of Constraint Satisfaction with Parametrization for Thermochemistry, Thermochemical Kinetics, and Noncovalent Interactions. *J. Chem. Theory Comput.* **2006**, *2*, 364–382. https://doi.org/10.1021/ct0502763.
38. Galano, A.; Alvarez-Idaboy, J.R. Kinetics of Radical-Molecule Reactions in Aqueous Solution: A Benchmark Study of the Performance of Density Functional Methods. *J. Comput. Chem.* **2014**, *35*, 2019–2026. https://doi.org/10.1002/jcc.23715.
39. Zhao, Y.; Truhlar, D.G. How Well Can New-Generation Density Functionals Describe the Energetics of Bond-Dissociation Reactions Producing Radicals? *J. Phys. Chem. A* **2008**, *112*, 1095–1099. https://doi.org/10.1021/jp7109127.
40. Carreon-Gonzalez, M.; Vivier-Bunge, A.; Alvarez-Idaboy, J.R. Thiophenols, Promising Scavengers of Peroxyl Radicals: Mechanisms and Kinetics. *J. Comput. Chem.* **2019**, *40*, 2103–2110. https://doi.org/10.1002/jcc.25862.
41. Gotō, H.; Ōsawa, E. An Efficient Algorithm for Searching Low-Energy Conformers of Cyclic and Acyclic Molecules. *J. Chem. Soc. Perkin Trans. 2* **1993**, *2*, 187–198. https://doi.org/10.1039/P29930000187.
42. Goto, H.; Osawa, E. Corner Flapping: A Simple and Fast Algorithm for Exhaustive Generation of Ring Conformations. *J. Am. Chem. Soc.* **1989**, *111*, 8950–8951. https://doi.org/10.1021/ja00206a046.
43. Matsui, T.; Baba, T.; Kamiya, K.; Shigeta, Y. An Accurate Density Functional Theory Based Estimation of PKa Values of Polar Residues Combined with Experimental Data: From Amino Acids to Minimal Proteins. *Phys. Chem. Chem. Phys.* **2012**, *14*, 4181. https://doi.org/10.1039/c2cp23069k.
44. Galano, A.; Pérez-González, A.; Castañeda-Arriaga, R.; Muñoz-Rugeles, L.; Mendoza-Sarmiento, G.; Romero-Silva, A.; Ibarra-Escutia, A.; Rebollar-Zepeda, A.M.; León-Carmona, J.R.; Hernández-Olivares, M.A.; et al. Empirically Fitted Parameters for Calculating PKa Values with Small Deviations from Experiments Using a Simple Computational Strategy. *J. Chem. Inf. Model.* **2016**, *56*, 1714–1724. https://doi.org/10.1021/acs.jcim.6b00310.
45. Marenich, A.V.; Cramer, C.J.; Truhlar, D.G. Universal Solvation Model Based on Solute Electron Density and on a Continuum Model of the Solvent Defined by the Bulk Dielectric Constant and Atomic Surface Tensions. *J. Phys. Chem. B* **2009**, *113*, 6378–6396. https://doi.org/10.1021/jp810292n.
46. Rimarčík, J.; Lukeš, V.; Klein, E.; Ilčin, M. Study of the Solvent Effect on the Enthalpies of Homolytic and Heterolytic N–H Bond Cleavage in p-Phenylenediamine and Tetracyano-p-Phenylenediamine. *J. Mol. Struct. THEOCHEM* **2010**, *952*, 25–30. https://doi.org/10.1016/j.theochem.2010.04.002.